JMEPEG (2020) 29:5420–5427
https://doi.org/10.1007/s11665-020-05016-0

1059-9495/$19.00

Novel Porous Barium Titanate/Nano-bioactive Glass Composite with High Piezoelectric Coefficient for Bone Regeneration Applications

Babak Saeidi, Mohammad Reza Derakhshandeh, Mehdi Delshad Chermahini, and Ali Doostmohammadi

(Submitted April 24, 2020; in revised form June 14, 2020; published online August 14, 2020)

Recently, porous bioceramics are widely used in bone tissue engineering in order to the regeneration of damaged tissues. Piezoelectric effect in bone plays a very important role in bone regeneration. Therefore, the purpose of this study was the fabrication of porous barium titanate (BT)/nanobioglass (nBG) scaffold (vol.% BT = 75% and 90%) with high piezoelectric coefficient by freeze casting technique. For this purpose, BT and nBG powders were synthesized using solid-state and sol–gel methods, respectively. Partial recrystallization of nBG phase during sintering process occurred. The highly oriented lamellar microstructure of the fabricated BT90/nBG10 scaffold with open/interconnected porosities observed. The BT75/nBG25 composite scaffold exhibited higher value of density (1.18 ± 0.1 g/cm^3) and lower amount of porosities (77 ± 1%) compared to the BT90/nBG10 scaffold (0.99 ± 0.1 g/cm^3 and 82 ± 1%). The piezoelectric coefficients of the BT90/nBG10 and BT75/nBG25 composite scaffolds obtained 36 pC/N and 24 pC/N which were much higher than that of the natural human bone. The BT75/nBG25 scaffold showed more compressive strength (16.9 ± 1.1 MPa) than that of BT90/nBG10 composite scaffold (8.1 ± 0.3 MPa). The MTT results after 24, 72 and 168 h of culture showed that both composites had acceptable cell viability and cells were able to adhere, proliferate and migrate into pores of the scaffolds. Furthermore, cell density and adhesion were little bit higher in the BT75/nBG25 composite. These results indicated that highly porous barium titanate scaffolds have great potential in tissue engineering applications for bone tissue repair and regeneration.

Keywords barium titanate, nano-bioactive glass, piezoelectric, scaffold

1. Introduction

Porous bioceramics namely scaffolds are widely used in bone tissue engineering in order to the regeneration of damaged tissues due to their low solubility, chemical inertness and higher biocompatibility compared to metallic implants (Ref 1-3). These structures containing interconnected micro- or macro-porosities facilitating osseointegration and formation of connective tissue in the bone/implant interface especially for bioactive ceramics (Ref 4). Porosity characteristics play an important role in bone regeneration. The amount of interconnected porosities, morphology and orientation strongly affects cell penetration in porous ceramics and consequently bone formation (Ref 5). However, it should be noted that large size of porosities and high amount of porosities make the mechanical strength unsuitable for biomedical applications (Ref 6). It has been found that porous ceramics with micro-porosities have higher compressive strength in comparison with macro-porosities (Ref 7).

In a study, porous hydroxyapatite (HA) scaffold was fabricated using a two-step freeze casting method by Tang et al. (Ref 8). Compressive strength of 22.4 MPa was achieved for the fabricated scaffold that is close to bone strength which can be considered as a suitable material for bone restoration. Fabrication of composite scaffolds made of bioactive glass (BG) and gelatin matrix by sol–gel method was studied by Nadeem et al. (Ref 9). The results showed that the scaffolds with an average porosity of 170 μm were obtained, which has high ability of apatite formation. The main advantage of BG is its high rate of surface reactions, which results in rapid bonding with tissues (Ref 10). However, these materials have some limitations for use as monolithic parts such as low mechanical strength and fracture toughness (Ref 11). Therefore, the use of BG is not suitable for load-bearing applications. But high bioactivity of these materials made them a suitable case for use in bio-composites (Ref 12).

Bone regeneration in BG scaffolds with oriented microstructure was evaluated in vivo using a rat calvarial defect model by Liu et al. (Ref 13). The results showed that BG scaffolds with 50% porosity and pore size of 50-150 μm showed 55% of bone formation after 24 weeks. Another sample with 80% porosity showed 46% of bone formation after 24 weeks. The results show that both scaffolds can be suitable for bone tissue engineering. It has been shown that interconnected pores with average porosity diameter of 100 μm in scaffolds could be achieved for the amount of porosity higher than 50%. In this

Babak Saeidi and **Mehdi Delshad Chermahini**, Faculty of Engineering, Shahrekord University, Shahrekord, Iran; **Mohammad Reza Derakhshandeh**, Department of Ceramics, Materials and Energy Research Center (MERC), Tehran, Iran; **Ali Doostmohammadi**, Faculty of Engineering, Shahrekord University, Shahrekord, Iran; and Department of Mechanical Engineering, Lassonde School of Engineering, York University, Toronto, Canada. Contact e-mail: doost@yorku.ca.

condition, tissue growth within the pores and the bio-functionality of the porous scaffold can be facilitated (Ref 14).

Different techniques have been reported for fabricating bioactive glass scaffolds such as sol–gel (Ref 15), replication of polymeric foam (Ref 16), thermally bonding of particles or fibers (Ref 17) and freeze casting (Ref 18). Among these techniques, freezing casting process is an appropriate method for the production of scaffolds due to its oriented microstructure which results in increasing compressive strength of these structures (Ref 19). It has been reported that compressive strength of scaffolds with directional microstructure is higher than that of random-orientated microstructures (Ref 19).

Piezoelectric effect in bone containing an outer hard layer of collagen and soft internal tissue was discovered for the first time in 1957 by Fukada et al. (Ref 20). In this research, the direct and inverse piezoelectric effect of the bovine bone was proved. The linear relationship between the dipoles and the stress or electric field and strain is observed, which demonstrated the piezoelectric effect in the bovine bone. Piezoelectric coefficient of 0.7 pC/N has been observed in bone tissue (Ref 21). It has been proved that the piezoelectric effect in bone plays a very important role in bone regeneration (Ref 22). Therefore, the use of biocompatible piezoelectric materials can be useful for bone healing process. Barium titanate (BT) is one of the most widely used piezoelectric materials for biomedical applications due to its high biocompatibility and suitable piezoelectric property (Ref 23, 24).

Therefore, the use of bio-composites scaffolds containing a bioactive component (such as BG) and a piezoelectric component (such as BT) can be effective in improving the osseointegration process. Here, the most similar researches on the electrical and biological properties of piezoelectric bio-composites are discussed. In a recent study, HA/BT composite scaffold with different compositions and amount of porosities fabricated by freezing casting method (Ref 23). The sample containing 10 wt.% HA and 90 wt.% BT showed the highest compressive strength of 14.5 MPa and the lowest porosity of 57.4% compared to the other samples. The piezoelectric coefficient of 1.2 pC/N and 2.8 pC/N obtained for composite containing of 70 wt.% BT and 90 wt.% BT, respectively, which are higher than bone piezoelectric coefficient. Increasing the amount of solid load in the initial suspension leads to an increase in the piezoelectric coefficient in these composite scaffolds. No cell toxicity was observed for the prepared scaffolds in the MTT tests. Dense HA/BT composites were fabricated by Baxter et al. (Ref 25). Piezoelectric coefficient of 57.8 pC/N was observed in HA/BT composites. The composite biocompatibility was also demonstrated by biological tests. No indication of the cytotoxicity of HA/BT composite was observed. In the recent study, BT/akermanite composite scaffolds with the suitable piezoelectric coefficient for bone defect recovery were fabricated by freeze casting method (Ref 26). High d_{33} of 4 pC/N was obtained for the composite scaffold with 90 wt.% BT. MTT assay indicated that the prepared composite scaffolds have no cytotoxicity on the human bone marrow mesenchymal stem cells.

In the present work, biocompatible nBG/BT composite scaffold with high piezoelectric coefficient was fabricated by freeze casting method. The main goal of this study was to evaluate the microstructural, mechanical, piezoelectric coefficient and biocompatibility of the prepared scaffolds. The amount of BT phase was selected as high as possible in these composites because of two reasons. On the one hand, by increasing the amount of nBG phase, liquid phase increases during the sintering process, which fills the pores and changes the microstructure of the composite scaffold. On the other hand, a high amount of BT is required to achieve a high piezoelectric coefficient in the composites. The obtained results were compared with compact and cancellous bone.

2. Experimental

2.1 Materials Preparation

The solid-state method was used for synthesizing of BT powders. $BaCO_3$ (Merck, purity > 99%) and TiO_2 (Merck, purity > 99%) powders were used as starting materials. $BaCO_3$ and TiO_2 powders were mixed with equal molar ratio using planetary mill in polymeric jar and zirconia balls in acetone medium. The ball to powders mass ratio, rotation speed and milling time were 5:1, 150 rpm and 5 h, respectively. The mixed powders were dried at 55 °C during stirring and calcined at 1000 °C for 5 h and finally pulverized.

Nano-bioactive glass powders (nBG, 63 mol.% SiO_2, 28 mol.% CaO and 9 mol.% P_2O_5) were prepared by sol–gel method using 2 N HCl (Merck), $CaNO_3{\cdot}4H_2O$ (Sigma-Aldrich, 99%), $(C_2H_5O)_3PO$ (Sigma-Aldrich) and $Si(OC_2H_5)_4$ (Sigma-Aldrich, 99%) as reported by Fathi et al. (Ref 27).

2.2 Scaffold Fabrication

The prepared BT and nBG powders were mixed with different compositions using a Spex shaker mill. Deionized water, polyvinylalcohol (PVA) and ammonium polyacrylate (Dolapix CE64) were used as freezing agent, binder and dispersant, respectively. The prepared slurries were put into a cylindrical die and frozen at − 40 °C with a cooling rate of − 1 °C/min. After that, the frozen samples were freeze-dried at − 55 °C and pressure of 10^{-5} mbar for 48 h. Finally, the dried samples were sintered at 1250 °C for 2 h. The conditions of scaffolds fabrication are presented in Table 1.

2.3 Characterization

2.3.1 Phase Analysis. X-ray diffraction (XRD) analysis (Philips XPert System, Cu k_α) was performed for phase identification of the synthesized materials and sintered BT/nBG composite scaffold.

2.3.2 Microstructural Characterization. Microstructures of the synthesized powders, as well as porosity characteristics of the fabricated scaffolds, were analyzed by field emission scanning electron microscope (TESCAN MIRA3; Czech Republic).

2.4 Properties

2.4.1 Physical Properties. Density and total porosity of the fabricated scaffolds were measured according to the C-373 ASTM standard. Based on this standard, the samples were boiled in deionized water for 5 h and immersed for 24 h. Saturated and suspended weights of the samples were measured using a scale with an accuracy of 0.0001 g. Dry weights were also measured after heating of the specimens in an oven at 150 °C for 5 h. Apparent density and total porosity of the samples were calculated using Archimedes' principle.

Table 1 Freeze casting conditions and composition of the prepared samples

Sample	BT, vol.%	nBG, vol.%	Solid loading, vol.%	Cooling rate, °C/min	PVA, wt.%	Dolapix, wt.%
BT90/nBG10	90	10	25	1	1	0.5
BT75/nBG25	75	25	25	1	1	0.5

2.4.2 Mechanical Properties of the Fabricated Scaffolds. The compressive strength of the fabricated composite scaffolds was carried out using SANTAM-20 mechanical testing machine at a rate of 0.1 mm/min. The results of compressive strength were reported after 5 repetitions.

2.4.3 Piezoelectric Coefficient Measurement. In order to measure the piezoelectric constant (d_{33}), the sintered samples were electrically poled by applying the corona poling using the DC voltage of 14 kV at 110 °C for 30 min. The heights of cylindrical sintered ceramics were about 30 mm. The values of d_{33} were measured using a quasistatic d_{33} m (Berlincourt-type) with a frequency of 100 Hz.

2.4.4 Cell Viability and Adhesion. The MTT assay was conducted according to one of our previous studies (Ref 28). All experiments were conducted for at least 5 times. To evaluate cell viability of the specimens, each sample was exposed to ethanol overnight, then sterilized for 3 h by UV irradiation, and then washed three times with phosphate-buffered saline (PBS). Thiazolyl blue tetrazolium bromide (MTT, Sigma, M5655) is dissolved in PBS at a concentration of 5 mg/ml and stored at 4 °C in a dark medium. Adult human mesenchymal stem cells (hMSC, Lonza Walkersville Inc., MD, USA) were used in this analysis. The cells were cultured at cell number of 1.3×10^4 cells/well in 24-well plates and stored for 24 and 72 and 168 h in an incubator at 37 °C and 90% humidity (RPMI 1640 medium containing 10% fetal bovine serum (FBS) and 1% Pen Strep). After that, the medium was removed and 100 ml of culture medium solution containing 10% of MTT was added to each well and incubated for 4 h in a dark medium at 37 °C. Then, the MTT medium was removed and 100 µL of dimethyl sulfoxide (DMSO, Merck) was added to the medium. After 15 min, the solution was analyzed by ELISA reader at a wavelength of 570 nm. The morphologies of hMSCs seeded on the samples were observed by SEM.

3. Results and Discussion

3.1 Microstructure and Characterization

Figure 1 shows the FESEM image of the synthesized nBG powders. Based on the micrograph, it is observable that particle sizes of the synthesized powders are less than 50 nm which is closely similar to the other similar studies (Ref 27, 29). XRD patterns of the synthesized BT powders as well as BT90/nBG10 scaffold are illustrated in Fig. 2. A single phase of barium titanate with tetragonal crystal system is characterized according to JCPDS# 01-079-2264. It can be observed that high levels of noise appear in the XRD pattern of the fabricated scaffold comparing to synthesized BT. The significant amount of noise may be due to the existence of the nBG powders as an amorphous phase. Besides, the minor values of additional phases such as cristobalite (SiO_2), Ca_3SiO_5, $CaSiO_3$ and

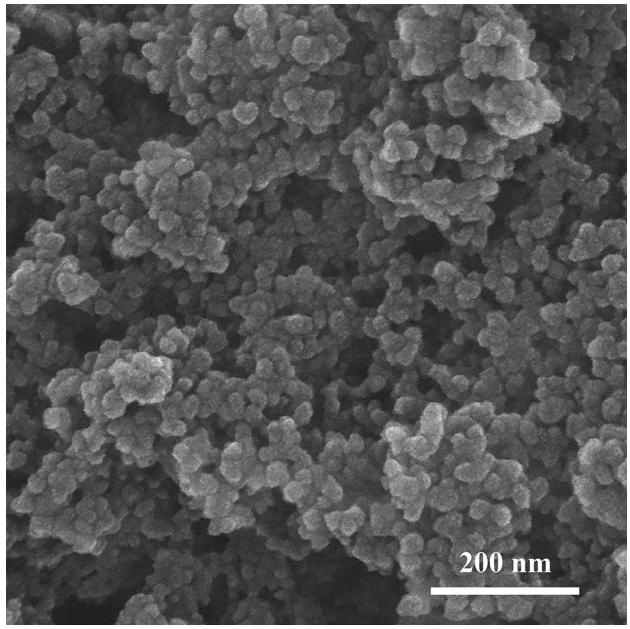

Fig. 1 FESEM image of the synthesized nBG powders

$Si_6Ca_5P_2O_{32}$ are observed due to the recrystallization of nBG via sintering process. The formation of these phases should not be considered as the occurrence of reaction between nBG and BT.

Figure 3 shows the typical FESEM micrographs of the sintered BT90/nBG10 composite scaffold. The highly oriented lamellar microstructure of the fabricated scaffold with open/interconnected porosities is clearly seen in the FESEM images of this sample. The average length and width of pores in this sample were about 158 ± 35 and 47 ± 11 µm, respectively. In the freeze-drying process, the solvent crystals are sublimated, leading to formation of lamellar pore channels. Similar microstructures are reported for freeze casting of different materials (Ref 30-32). FESEM images of the sintered BT75/nBG25 composite scaffold recorded at different magnifications are shown in Fig. 4. The microstructure of BT75/nBG25 composite scaffold with inhomogeneous cellular porosities as well as dense areas is observed. Mean size of porosities in this sample was about 112 ± 48 µm. Several parameters such as solid loading, freezing rate, rheology of suspension, pH could affect the microstructure of the freeze-dried scaffolds (Ref 19). Although the mentioned parameters are constant for both samples, different microstructures of the scaffolds are observed. Deville et al. (Ref 33) reported that sintering conditions affect the microstructure as well as the total porosity of scaffolds. The only variable parameter in this study is amount of the nBG phase. It is suggested that by increasing the amount of nBG phase, the liquid phase increased during the sintering process,

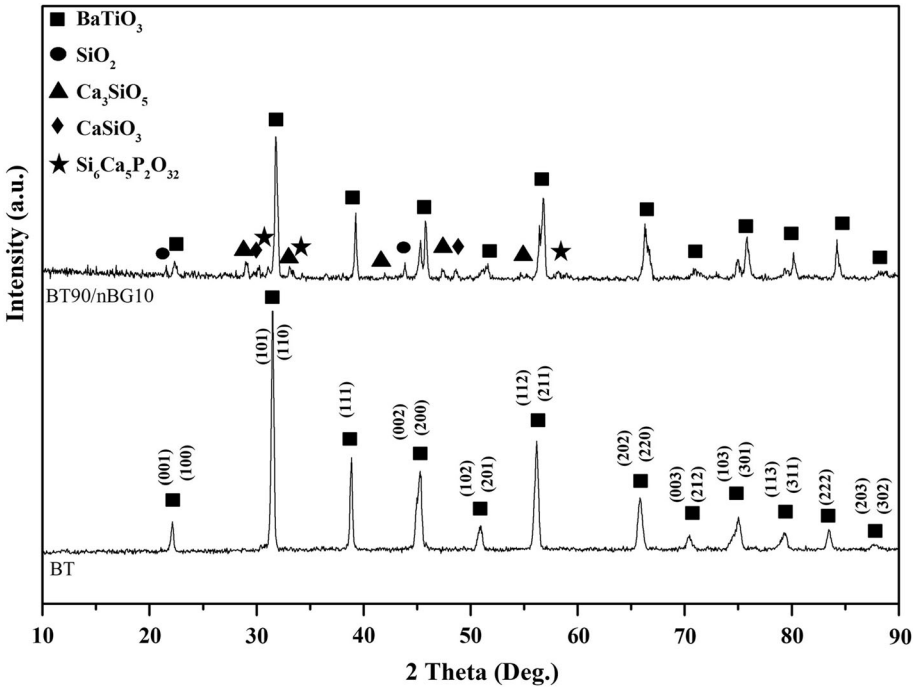

Fig. 2 XRD pattern of the synthesized BT powders and sintered BT90/nBG10 composite scaffold

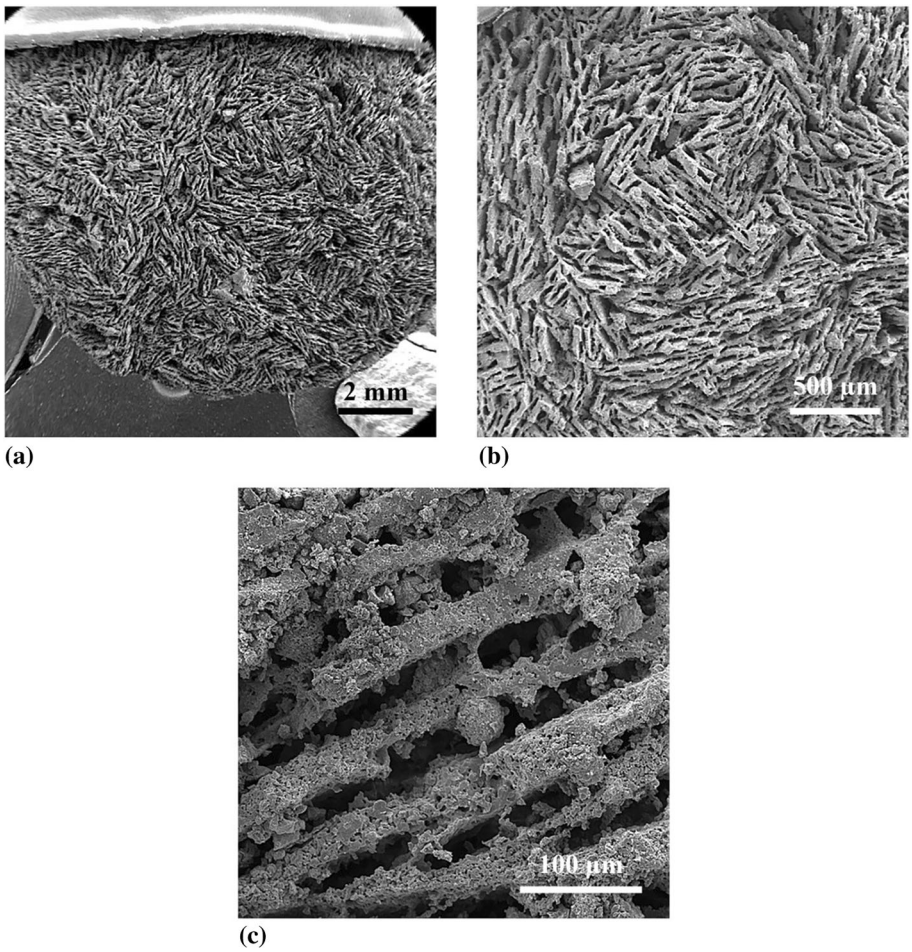

Fig. 3 Typical FESEM micrographs of the sintered BT90/nBG10 composite scaffold recorded at different magnifications

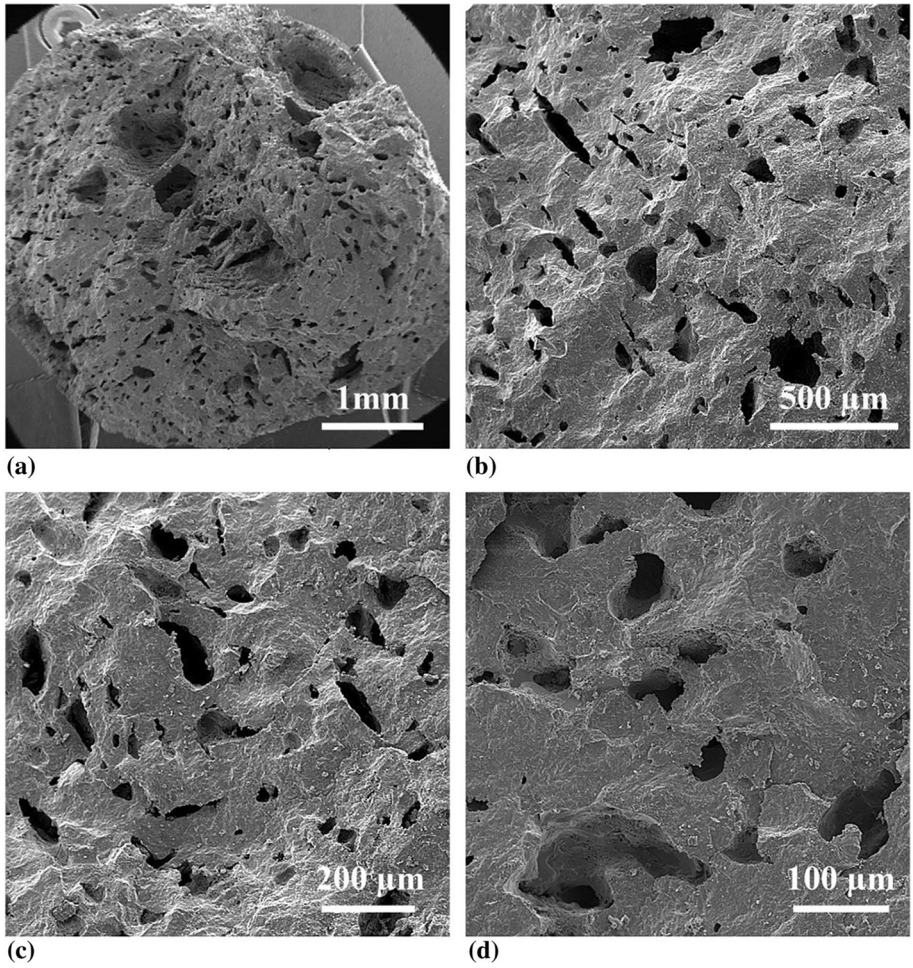

Fig. 4 FESEM images of the sintered BT75/nBG25 composite scaffold recorded at different magnifications

which fills the pores and changes the microstructure of the composite scaffold. As mentioned above, in hard tissue engineering, morphology, size and the type of porosities in implants are important factors for bone regeneration. Interconnected porosities facilitating osseointegration and formation of connective tissue in the bone/implant interface. The amount of interconnected porosities, morphology and orientation strongly affects cell penetration in porous ceramics and consequently bone formation (Ref 5). Therefore, it is suggested that the microstructure of BT90/nBG10 sample could have higher osseointegration ability than that of BT75/nBG25 sample.

3.2 Physical Properties

Density and porosity results of the sintered composite scaffolds are presented in Table 2. It is obvious that the BT75/nBG25 composite scaffold exhibited the higher value of density (1.18 ± 0.1 g/cm^3) and accordingly the lower amount of porosities ($77 \pm 1\%$) compared to the BT90/nBG10 scaffold (0.99 ± 0.1 g/cm^3 and $82 \pm 1\%$). This behavior may be a consequence of more liquid-phase formation for BT75/nBG25 sample during the sintering process. Comparing the density and porosity results of the samples shows that the obtained density and porosity values of fabricated composite scaffolds are close to the cancellous bone (0.8-1.1 g/cm^3 and 75-90%) (Ref 26, 34, 35).

3.3 Piezoelectric Coefficient

The piezoelectric properties of the BT90/nBG10 and BT75/nBG25 composite scaffolds are presented in Table 2. As expected, by increasing the amount of BT in composites, the piezoelectric coefficient of the fabricated scaffolds increased. This can be due to the presence of BT which is a piezoelectric material with an asymmetric perovskite crystal structure. This means the higher value of d_{33} for BT90/nBG10 (36 pC/N) comparing to BT75/nBG25 composite scaffold (24 pC/N). The obtained d_{33} values of both composite scaffolds were much higher than that of the natural human bone (0.7 pC/N) (Ref 21) which could facilitate bone regeneration. Generally, in a porous piezoceramic with dense walls, the piezoelectric coefficient could be improved by increasing the size of porosities. This can be due to decreasing surface area and defects. The effect of porosity size and orientation on the piezoelectric properties of PZT scaffolds fabricate by freezing casting method was investigated by Guo et al. (Ref 36). In their study, it has been shown that porosity size and orientation have a significant effect on its piezoelectric coefficient. In their study, a higher piezoelectric coefficient was obtained for the fabricated scaffold with mean pore size of 40 µm than the scaffold with mean pore size of 25 µm. Although the volume fraction of the porosities in the fabricated scaffolds was above 60%, the piezoelectric coefficient of the scaffolds was between 81 and 93% of its theoretical value (Ref 36).

Table 2 Comparison between fabricated scaffolds and bone for the piezoelectric coefficient, physical and mechanical properties

Property	BT90/nBG10	BT75/nBG25	Compact bone	Cancellous bone
Density, g/cm^3	0.99 ± 0.1	1.18 ± 0.1	1.4-1.9	0.8-1.1
Porosity, %	82 ± 1	77 ± 1	5-30	75-95
Compressive strength, MPa	8.1 ± 0.3	16.9 ± 1.1	50-150	1.3-13
d_{33}, pC/N	36	24	0.7	0.7

Statistical analysis was conducted using ANOVA; $P \leq 0.001$ (Differences were considered significant for $P \leq 0.05$)

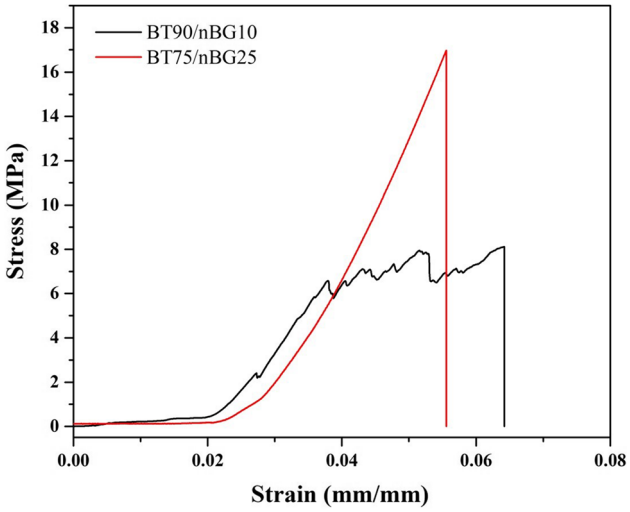

Fig. 5 Compressive stress vs. strain plots of the fabricated BT90/nBG10 and BT75/nBG25 composite scaffolds

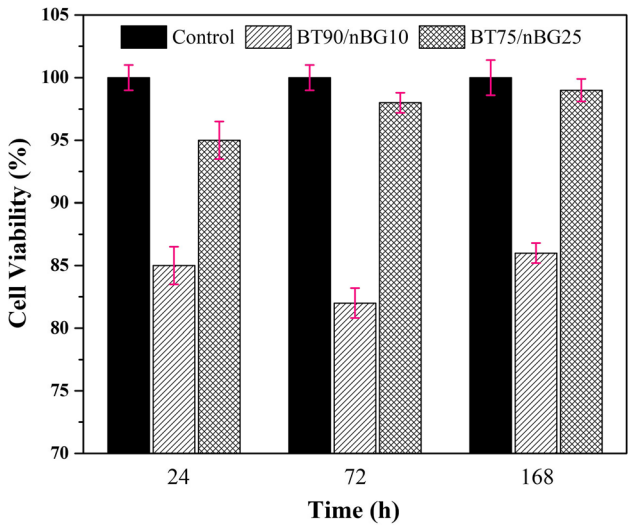

Fig. 6 Viability of hMSCs on the BT75/nBG25 and BT90/nBG10 composite scaffolds after 24, 72 and 168 h of culture; Differences were significant for $P \leq 0.01$

3.4 Mechanical Properties

Figure 5 reveals the compressive stress versus strain plots of the fabricated BT90/nBG10 and BT75/nBG25 composite scaffolds. As can be seen, the BT75/nBG25 scaffold showed more compressive strength (16.9 ± 1.1 MPa) than that of BT90/nBG10 composite scaffold (8.1 ± 0.3 MPa). The BT75/nBG25 composite scaffold showed linear stress–strain behavior, while the BT90/nBG10 composite scaffold showed fluctuations in its stress–strain diagram. This may be due to different morphologies of the composite scaffolds. As shown in Fig. 4, the BT75/nBG25 composite has high density in the walls (dense areas) with cellular porosities; while the BT90/nBG10 composite scaffold showed a lamellar microstructure. Therefore, these fluctuations can be due to the gradual degradation of the layers. The obtained results of compressive strength of the fabricated composite scaffolds are in the range of cancellous bone (1.3-13 MPa) (Ref 37) as indicated in Table 2.

3.5 Cytotoxicity Evaluation

According to ISO 10993-5 standard, reduction of cell viability by more than 30% is considered a cytotoxic effect. The MTT results after 24, 72 and 168 h of culture showed that both composite samples had acceptable cell viability. As indicated in Fig. 6, the viability of hMSCs on the BT75/nBG25 composite scaffold is more than 98% (P value < 0.05). The BT90/nBG10 composite scaffold also had no toxicity since cell viability after 1 week was more than 82%. There is no significant difference between cell viability over the time ($P > 0.05$) in BT90/nBG10 composition. Increasing the amount of nBG phase in BT75/nBG25 composite leads to increase the viability of hMSCs, which is completely expected.

The morphology of hMSCs on the surface can directly reflect the biological activity of the material (Ref 24, 28). Figure 7 shows the growth and adhesion of hMSCs on the surface of BT/nBG piezoelectric bioceramics. hMSCs are polygonal and distributed on the material surface, and the pseudopodium is connected with piezoelectric bioceramics and neighboring cells. The cells associated with each sample showed excellent growth, including good cell morphology, extracellular secretions and intercellular connections. Bioactive glass (BG) is a widely used bone substitute material, and its biological activity is generally recognized (Ref 10, 11). hMSCs showed a better adhesion on BT75/nBG25 composite sample (Fig. 7a). This result was completely expected because of the higher percentage of BG in this composition (Ref 7-11). These results indicate that the BT75/nBG25 composite scaffold with improved mechanical and biological properties and high piezoelectric coefficient could be potentially a suitable candidate for hard tissue engineering and bone defect recovery. More investigations including in vivo studies and further mechanical properties of the composites are ongoing.

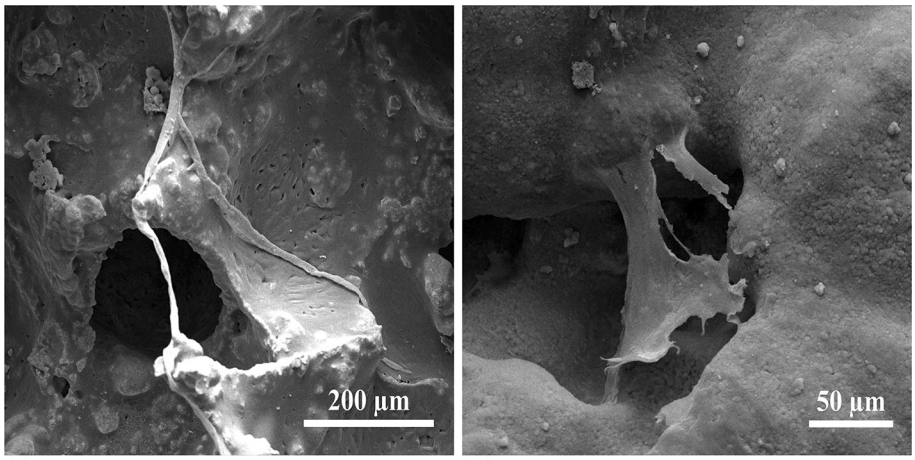

Fig. 7 Growth and adhesion of hMSCs on the surface of BT/nBG piezoelectric composites: (a) BT75/nBG25 and (b) BT90/nBG10

4. Conclusions

In this study, BT/nBG piezoelectric scaffolds (vol.% BT = 75% and 90%) as a potential candidate for bone replacement with high d_{33} were fabricated using freeze casting technique. For this purpose, BT and nBG powders were successfully synthesized using solid-state and sol–gel methods, respectively. The occurrence of partial recrystallization of nBG caused by sintering treatment was observed. The BT90/nBG10 composite scaffold showed oriented lamellar morphology and open/interconnected porosities; while BT75/nBG25 sample exhibited cellular porosities with dense walls. It was suggested that by increasing the amount of nBG phase, the liquid phase increased during the sintering process, which fills the pores and changes the microstructure of the composite scaffold. The BT75/nBG25 composite scaffold exhibited higher value of density (1.18 ± 0.1 g/cm^3) and lower amount of porosities ($77 \pm 1\%$) compared to the BT90/nBG10 scaffold (0.99 ± 0.1 g/cm^3 and $82 \pm 1\%$). This phenomenon may be due to higher liquid-phase formation of BT75/nBG25 sample during the sintering process. The resultant piezoelectric constants for the BT90/nBG10 and BT75/nBG25 composite scaffolds were remarkably higher than natural human bone, which could facilitate osseointegration. As expected, higher value of d_{33} for BT90/nBG10 (36 pC/N) comparing to BT75/nBG25 composite scaffold (24 pC/N) was obtained. The BT75/nBG25 scaffold showed more compressive strength (16.9 ± 1.1 MPa) than that of BT90/nBG10 composite scaffold (8.1 ± 0.3 MPa). The BT75/nBG25 composite scaffold showed linear stress–strain behavior, while the BT90/nBG10 sample revealed fluctuations in its stress–strain diagram. This may be caused by different morphologies of the fabricated scaffolds. Comparing the density and porosity results of the samples shows that the obtained density and porosity values of fabricated composite scaffolds are close to cancellous bone. The MTT results after 24, 72 and 168 h of culture showed that both composite samples had acceptable cell viability. In addition, increasing the amount of nBG phase leading to increase the viability of hMSCs up to 98%.

References

1. B. Gaihre and A.C. Jayasuriya, Comparative Investigation of Porous Nano-hydroxyapaptite/Chitosan, Nano-Zirconia/Chitosan and Novel Nano-calcium Zirconate/Chitosan Composite Scaffolds for Their Potential Applications in Bone Regeneration, *Mater. Sci. Eng., C*, 2018, **91**, p 330–339
2. M.R. Derakhshandeh, M.J. Eshraghi, M.M. Hadavi, M. Javaheri, S. Khamseh, M.G. Sari et al., Diamond-Like Carbon thin FILMS Prepared by pulsed-DC PE-CVD for Biomedical Applications, *Surf. Innov.*, 2018, **6**, p 167–175
3. S.M.R. Derakhshandeh, M.J. Eshraghi, M. Javaheri, S. Khamseh, M.G. Sari, P. Zarrintaj et al., Diamond-Like Carbon-Deposited Films: a New Class of Bio-Corrosion Protective Coatings, *Surf. Innov.*, 2018, **6**, p 266–276
4. J.N. Harvestine, N.L. Vollmer, S.S. Ho, C.A. Zikry, M.A. Lee, and J.K. Leach, Extracellular Matrix-Coated COMPOSITE scaffolds Promote mesenchymal Stem Cell Persistence and Osteogenesis, *Biomacromol*, 2016, **17**, p 3524–3531
5. L. Stipniece, I. Narkevica, M. Sokolova, J. Locs, and J. Ozolins, Novel Scaffolds Based on Hydroxyapatite/Poly (VINYL alcohol) Nanocomposite Coated Porous TiO2 Ceramics for Bone Tissue Engineering, *Ceram. Int.*, 2016, **42**, p 1530–1537
6. B. Chang, W. Song, T. Han, J. Yan, F. Li, L. Zhao et al., Influence of Pore Size of Porous Titanium Fabricated by Vacuum Diffusion Bonding of Titanium Meshes on Cell Penetration and Bone Ingrowth, *Acta Biomater.*, 2016, **33**, p 311–321
7. D.-M. Liu, Influence of Porosity and Pore Size on the Compressive Strength of Porous Hydroxyapatite Ceramic, *Ceram. Int.*, 1997, **23**, p 135–139
8. Y. Tang, K. Zhao, L. Hu, and Z. Wu, Two-Step Freeze Casting Fabrication of Hydroxyapatite Porous Scaffolds with Bionic Bone Graded Structure, *Ceram. Int.*, 2013, **39**, p 9703–9707
9. D. Nadeem, M. Kiamehr, X. Yang, and B. Su, Fabrication and In vitro Evaluation of a Sponge-Like Bioactive-Glass/Gelatin Composite Scaffold for Bone Tissue Engineering, *Mater. Sci. Eng., C*, 2013, **33**, p 2669–2678
10. Z. Khurshid, S. Husain, H. Alotaibi, R. Rehman, M.S. Zafar, I. Farooq et al., *Novel Techniques of Scaffold Fabrication for Bioactive Glasses*, Elsevier, Amsterdam, 2019, p 497–519
11. G. Kaur, V. Kumar, F. Baino, J.C. Mauro, G. Pickrell, I. Evans et al., Mechanical Properties of Bioactive Glasses, Ceramics, Glass-Ceramics and Composites: State-of-the-Art Review and Future Challenges, *Mater. Sci. Eng. C*, 2019, **104**, p 109895
12. A. Motealleh, S. Eqtesadi, F.H. Perera, A.L. Ortiz, P. Miranda, A. Pajares et al., Reinforcing 13–93 Bioglass Scaffolds Fabricated by Robocasting and Pressureless Spark Plasma Sintering with Graphene Oxide, *J. Mech. Behav. Biomed. Mater.*, 2019, **97**, p 108–116

13. X. Liu, M.N. Rahaman, and Q. Fu, Bone Regeneration in Strong Porous Bioactive Glass (13-93) Scaffolds with an Oriented Microstructure Implanted in Rat Calvarial Defects, *Acta Biomater.*, 2013, **9**, p 4889–4898
14. T.M. Freyman, I.V. Yannas, and L.J. Gibson, Cellular Materials as Porous Scaffolds for Tissue Engineering, *Prog. Mater Sci.*, 2001, **46**, p 273–282
15. F. Baino, E. Fiume, M. Miola, F. Leone, B. Onida, and E. Verné, Fe-Doped Bioactive Glass-Derived Scaffolds produced by Sol-Gel foaming, *Mater. Lett.*, 2019, **235**, p 207–211
16. S. Cabanas-Polo, A. Philippart, E. Boccardi, J. Hazur, and A.R. Boccaccini, Facile Production of Porous Bioactive Glass Scaffolds by the Foam Replica Technique Combined with Sol–Gel/Electrophoretic Deposition, *Ceram. Int.*, 2016, **42**, p 5772–5777
17. Q. Fu, E. Saiz, M.N. Rahaman, and A.P. Tomsia, Bioactive Glass Scaffolds for Bone Tissue Engineering: State of the Art and Future Perspectives, *Mater. Sci. Eng., C*, 2011, **31**, p 1245–1256
18. D.M.M. dos Santos, S.M. de Carvalho, M.M. Pereira, M. Houmard, and E.H.M. Nunes, Freeze-Cast Composite Scaffolds Prepared from Sol-Gel Derived 58S Bioactive Glass and Polycaprolactone, *Ceram. Int.*, 2019, **45**, p 9891–9900
19. K.L. Scotti and D.C. Dunand, Freeze Casting–A Review of Processing, Microstructure and Properties Via the Open Data Repository, FreezeCasting. net, *Prog. Mater. Sci.*, 2018, **94**, p 243–305
20. E. Fukada and I. Yasuda, On the Piezoelectric Effect of Bone, *J. Phys. Soc. Jpn.*, 1957, **12**, p 1158–1162
21. J. Park and R.S. Lakes, *Biomaterials: An Introduction*, Springer, Berlin, 2007
22. F. Jianqing, Y. Huipin, and Z. Xingdong, Promotion of Osteogenesis by a Piezoelectric Biological Ceramic, *Biomaterials*, 1997, **18**, p 1531–1534
23. Y. Zhang, L. Chen, J. Zeng, K. Zhou, and D. Zhang, Aligned Porous Barium Titanate/Hydroxyapatite Composites with High Piezoelectric Coefficients for Bone Tissue Engineering, *Mater. Sci. Eng., C*, 2014, **39**, p 143–149
24. A. Ehterami, M. Kazemi, B. Nazari, P. Saraeian, and M. Azami, Fabrication and Characterization of Highly Porous Barium Titanate Based Scaffold Coated by Gel/HA Nanocomposite with High Piezoelectric Coefficient for Bone Tissue Engineering Applications, *J. Mech. Behav. Biomed. Mater.*, 2018, **79**, p 195–202
25. F.R. Baxter, I.G. Turner, C.R. Bowen, J.P. Gittings, and J.B. Chaudhuri, An In Vitro Study of Electrically Active Hydroxyapatite-Barium Titanate Ceramics Using Saos-2 Cells, *J. Mater. Sci. Mater. Med.*, 2009, **20**, p 1697–1708
26. H. Shokrollahi, F. Salimi, and A. Doostmohammadi, The Fabrication and Characterization of Barium Titanate/Akermanite Nano-bio-ceramic with a Suitable Piezoelectric Coefficient for Bone Defect Recovery, *J. Mech. Behav. Biomed. Mater.*, 2017, **74**, p 365–370
27. M.H. Fathi and A. Doostmohammadi, Preparation and Characterization of Sol–Gel Bioactive Glass Coating for Improvement of Biocompatibility of Human Body Implant, *Mater. Sci. Eng., A*, 2008, **474**, p 128–133
28. S.M.R. Derakhshandeh, S.M.M. Hadavi, M.J. Eshraghi, M. Javaheri, and M. Mozafari, Improved Electrochemical Performance of Nitrocarburised Stainless Steel by Hydrogenated Amorphous Carbon Thin Films for Bone Tissue Engineering, *IET Nanobiotechnol.*, 2017, **11**, p 656–660
29. K. Zheng and A.R. Boccaccini, Sol-gel Processing of Bioactive Glass Nanoparticles: A Review, *Adv. Colloid Interface Sci.*, 2017, **249**, p 363–373
30. Y. Liu, N. Fang, B. Liu, L. Song, B. Wen, and D. Yang, Aligned Porous Chitosan/Graphene Oxide Scaffold for Bone Tissue Engineering, *Mater. Lett.*, 2018, **233**, p 78–81
31. S. Algharaibeh, A.J. Ireland, and B. Su, Bi-directional Freeze Casting of Porous Alumina Ceramics: A Study of the Effects of Different Processing Parameters on Microstructure, *J. Eur. Ceram. Soc.*, 2019, **39**, p 514–521
32. Y. Tang, S. Qiu, Q. Miao, and C. Wu, Fabrication of Lamellar Porous Alumina with Axisymmetric Structure by Directional Solidification with Applied Electric and Magnetic Fields, *J. Eur. Ceram. Soc.*, 2016, **36**, p 1233–1240
33. S. Deville, E. Saiz, and A.P. Tomsia, Freeze castiNg of Hydroxyapatite Scaffolds for Bone Tissue Engineering, *Biomaterials*, 2006, **27**, p 5480–5489
34. P.L. Blanton and N.L. Biggs, Density of Fresh and Embalmed Human Compact and Cancellous Bone, *Am. J. Phys. Anthropol.*, 1968, **29**, p 39–44
35. R. Hodgskinson, C.F. Njeh, M.A. Whitehead, and C.M. Langton, The Non-linear Relationship Between BUA and Porosity in Cancellous Bone, *Phys. Med. Biol.*, 1996, **41**, p 2411
36. R. Guo, C.-A. Wang, and A. Yang, Effects of Pore Size and Orientation on Dielectric and Piezoelectric Properties of 1-3 Type Porous PZT Ceramics, *J. Eur. Ceram. Soc.*, 2011, **31**, p 605–609
37. M. Martens, R. Van Audekercke, P. Delport, P. De Meester, and J.C. Mulier, The Mechanical Characteristics of Cancellous Bone at the Upper Femoral Region, *J. Biomech.*, 1983, **16**, p 971–983